Conduction-band structure of $Bi_{2-x}Sb_xSe_3$ mixed crystals by Shubnikov−de Haas and cyclotron resonance measurements in high magnetic fields

V. A. Kulbachinskii

Low Temperature Physics Department, Moscow State University, 119899 Moscow, Russia

N. Miura, H. Nakagawa, H. Arimoto, and T. Ikaida

Institute for Solid State Physics, University of Tokyo, Roppongi, Minato-ku, Tokyo, Japan

P. Lostak and C. Drasar

University of Pardubice, 53210 Pardubice, Czech Republic

The conduction-band structure of single crystals $Bi_{2-x}Sb_xSe_3$ ($0 \leq x \leq 0.52$) was investigated in high magnetic fields by the Shubnikov−de Haas (SdH) effect (up to 40 T) and cyclotron resonance (up to 150 T). Signals from two conduction bands were detected in both experiments. The anisotropy of the Fermi surface and the effective masses for magnetic fields $B \parallel c$ and $B \perp c$ were determined for different x. It was found that the cyclotron masses for $B \parallel c$ in the upper and lower conduction bands do not depend on temperature or electron concentration. The temperature dependence of the resistivity, the Hall effect, and the Seebeck coefficient have been measured as functions of Sb concentration x. The free-electron concentration was found to be suppressed by the incorporation of Sb into Bi_2Se_3 crystals. [S0163-1829(99)03623-1]

I. INTRODUCTION

Solid solutions based on narrow-gap layered semiconductor Bi_2Se_3 (as well as Sb_2Te_3, Bi_2Te_3) with the tetradymite structure are important materials for applications as thermoelectric devices.[1,2] Considerable attention has been devoted to investigation of the energy spectrum of Bi_2Se_3.[3–6] Horak *et al.* investigated the influence of doping of Cd,[7] and Novotny, Lostak, and Horak studied the effect of In doping[8] on transport and optical properties. Recently, systematic studies have been made on mixed crystals based on Bi_2Se_3 (Refs. 9 and 10) and Sb_2Se_3.[11] Kohler[3] determined the conduction-band parameters of Bi_2Se_3 from the Shubnikov−de Haas (SdH) effect for electron concentrations ranging between 4×10^{17} and 4×10^{19} cm^{-3}. It was experimentally shown that the Fermi surface in n-Bi_2Se_3 is approximately an ellipsoid of rotational symmetry around the c_3 axis with a small amount in of trigonal warping. The $E(k)$ dispersion is parabolic in the direction perpendicular to the c_3 axis for $k_c = 0$, but considerably nonparabolic in the parallel direction.[4] The parameters of the nonparabolic $E(k)$ relation caused by the k^4 term were obtained by a comparison with numerical calculations of the extremal cross sections of the Fermi surface and the corresponding reciprocal SdH periods.[5] High magnetic-field data for low quantum numbers in a pulsed field B up to 35 T ($B \parallel c_3$) revealed an influence of spin splitting which causes a shift of the resistivity extrema. No spin splitting in the SdH resistivity extrema was observed at high quantum numbers.[6] Calculation of the band structure of Bi_2Te_3 was carried out by several authors.[12–14] The common crystal structure of Bi_2Se_3 and Bi_2Te_3 is responsible for the similarity of their electron energy band structure. However, the differences in the lattice constant and the atomic potential should result in some differences between the two crystals.

According to Oleshko and Korolyshin,[15] the principal minimum of the conduction band in Bi_2Se_3 is located at the center of the Brillouin zone (Γ point), and therefore it can be represented by one ellipsoid. This is in contrast to Bi_2Te_3 in which the conduction band has two extrema with six-ellipsoidal sets.

There have been only few reports on the physical properties of the mixed crystals Bi_2Se_3-Sb_2Se_3. Substitution of Bi by Sb in Bi_2Se_3 is possible only in the concentration range of 0–16.2 mol % Sb.[16] In the present paper, we study the energy-band structure of $Bi_{1-x}Sb_xSe_3$ mixed crystals by the SdH effect and cyclotron resonance. The SdH effect was investigated in single crystals of $Bi_{1-x}Sb_xSe_3$ ($0 \leq x \leq 0.52$) in the temperature range 1.4–4.2 K and in pulsed magnetic fields up to 40 T. The temperature dependence of the resistivity and the Hall effect in a lower field range were measured in a wide range of temperature, $4.2 \leq T \leq 300$ K. The cyclotron resonance measurements were performed in the same samples at very high magnetic fields up to 150 T. Owing to the high field, clean cyclotron resonance spectra were observed in this class of crystals. From the analysis of the overall experimental data we obtained the effective masses of the conduction band.

II. EXPERIMENTAL PROCEDURE

$Bi_{2-x}Sb_xSe_3$ ($0 < x < 0.52$) single crystals were grown by the Bridgman method. The starting polycrystalline substances were synthesized from elements Bi, Sb, and Se with 5 N purity in evacuated conical silica ampoules at 773 °C for 48 h. The growth of single crystals was carried out in the same ampoule with a pulling rate of 1.3 mm/h. The composition of samples was determined by an energy disperse x-ray analyzer Kewex Delta 5 with a quantum detector. The energy spectra were recorded under the following conditions:

TABLE I. Resistivity $\rho^{4.2}$ and ρ^{300}, mobility $\mu^{4.2}$ and μ^{300} at $T = 4.2$ K and $T = 300$ K, and Hall coefficient R_H at 4.2, 77, and 300 K for $Bi_{2-x}Sb_xSe_3$ single-crystal samples.

N	Sb content X	$\rho^{4.2}$ (mΩ cm)	ρ^{300} (mΩ cm)	$R_H^{4.2}$ (cm³/C)	R_H^{77} (cm³/C)	R_H^{300} (cm³/C)	$\mu^{4.2}$ (m²/Vs)	μ^{300} (m²/Vs)
1	0	0.15	0.39	0.17	0.16	0.18	0.11	0.046
2	0.02	0.14	0.30	0.15	0.11	0.16	0.107	0.053
3	0.06	0.17	0.36	0.24	0.16	0.17	0.14	0.047
4	0.2	0.18	0.39	0.30	0.15	0.18	0.167	0.046
5	0.29	0.25	0.70	0.50	0.21	0.26	0.20	0.037
6	0.45	0.26	0.79	0.60	0.30	0.35	0.23	0.044
7	0.52	0.27	0.80	0.74	0.44	0.50	0.31	0.064

accelerating voltage of the primary beam is 20 kV; the energy scale is divided into 1000 channels (10 eV per channel); the detector sensitivity is 140 eV; the detector is placed at an angle of 30° with respect to the sample surface. The single crystals were cleaved with cleaved surfaces perpendicular to the c_3 axis (perpendicular to the layers) and then cut by a spark erosion machine to a size $0.7 \times 0.7 \times 5$ mm³. The resistivity and the Hall effect were measured by a conventional four-probe method with a dc current along the c_2 axis in magnetic fields up to 8 T applied along the c_3 axis, using a superconducting solenoid.

The Shubnikov−de Haas effect was measured with a current J applied along the c_2 axis for two orientations of magnetic field: $B\|c_3$ axis and $B\perp c_3$ axis $\perp J$. For investigating the SdH effect in higher fields, we used a pulse magnet which can produce a long pulse field (~ 20 ms duration) up to 40 T. A standard four-contact method was employed to measure the transverse magnetoresistance.

Cyclotron resonance was measured in high magnetic fields up to 150 T produced by the single turn coil technique.[17] A fast capacitor bank of 10 kJ (40 kV) was employed to supply short large pulsed currents of order of 2 MA to a small single turn coil. A very high field is directly produced by the large current. Although the coil explodes violently by a large electromagnetic force, high fields are generated before the coil destruction owing to a very short pulse duration (about 7 μs). One of the advantages of this technique is that samples and cryostats are not destroyed in spite of the destruction of the coil, so we can repeat the experiments on the same sample many times. A CO_2 laser was employed as the radiation source of the cyclotron resonance at wavelengths of 9–11 μm.[18] We employed a HgCdTe detector to detect the rapid change of the infrared radiation.

III. EXPERIMENTAL RESULTS

A. Resistivity, thermopower, and Hall effect

The Hall coefficient R_H, electrical resistivity, and mobility of samples at different temperatures are summarized in Table I. The temperature dependence of the resistivity for $Bi_{2-x}Sb_xSe_3$ with different x is shown in Fig. 1. When temperature is lowered, the resistivity ρ also decreases with a power law $\rho \sim T^m$, with $m \approx 1$. For $T < 100$ K the resistivity saturates. From such type of dependencies, we conclude that at $T > 100$ K the carrier scattering is predominantly governed

by phonons and impurities, while at lower temperatures the dominant scattering is by neutral impurities. The absolute value of the resistivity increases as x increases except sample N2 with $x = 0.02$. The Hall effect was investigated for three different temperatures: 300, 77, and 4.2 K. The dependence of the Hall coefficient on antimony content x is shown in Fig. 2. It evidently shows that the Hall coefficient R_H for magnetic fields $B\|c_3$ is a decreasing function of x in the region of small values of x, and then for larger values of x it starts increasing. Almost the same x dependence was observed for the Hall mobility at $T = 4.2$ K, as shown in Fig. 3.

The Seebeck coefficient α has been measured in $Bi_{2-x}Sb_xSe_3$ for the $\nabla T\|c_2$ at room temperature as a function of x. The experimental results are summarized in Table II. As it is seen in the table, the value of α decreases with increasing x at low concentrations of Sb and then starts increasing. The x dependence of α which is similar to the dependence of $R_H(x)$ can be explained by the change of electron concentration.

B. Shubnikov−de Haas effect

In all the samples, we observed a positive magnetoresistance reaching about 10% at 40 T. Figure 4 shows the oscillatory part of the magnetoresistance in some samples of $Bi_{2-x}Sb_xSe_3$ for B parallel to the c_3 axis as a function of the inverse magnetic field. The monotonous part of the magnetoresistance was subtracted to extract the oscillatory part. The Fourier transform of the oscillation is shown in Fig. 5. In
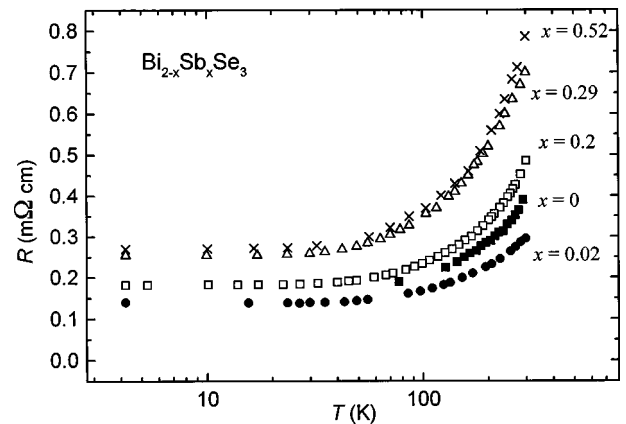

FIG. 1. Temperature dependence of resistivity for $Bi_{2-x}Sb_xSe_3$ samples with different Sb content in semilogarithmic scale.
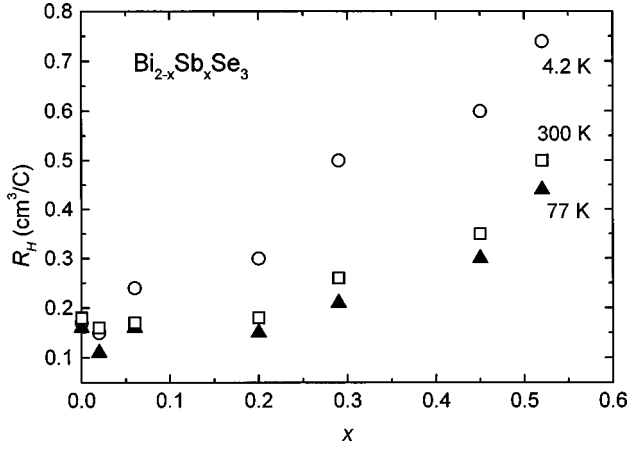
FIG. 2. Dependence of the Hall coefficient on antimony content x in $Bi_{2-x}Sb_xSe_3$ samples for 300, 77, and 4.2 K.

FIG. 3. Mobility of samples $Bi_{2-x}Sb_xSe_3$ as function of x at 4.2 K.

all the samples (except sample N7 $Bi_{1.48}Sb_{0.52}Se_3$ with the highest Sb concentration) a second frequency F_2 with a lower amplitude was found as marked by arrows in Fig. 5. Although there are two frequencies nearby, beats are imperceptible in the data of Fig. 4. The reason for the absence of beating is due to the very small amplitude of the second frequency F_2. The values of the main frequency F_1 and the second frequency F_2 decrease as x increases. The dependence of F_1 on x is shown in Table II. In the trace for $x = 0.52$, the second frequency was indiscernible, most probably due to the low amplitude of the oscillation. The anisotropy factor $\eta = S_{B\perp C}/S_{B\|C}$ of the Fermi surface and its dependence on electron concentration were also determined by high magnetic field measurements. Figure 6 shows the oscillatory part of the transverse magnetoresistance in a sample of $Bi_{1.48}Sb_{0.52}Se_3$ for two different orientations of magnetic fields, $B\|c_3$ axis and $B\perp c_3$ axis. It was found that the anisotropy strongly depends on carrier concentration which is proportional to $F_1^{3/2}$ as shown in Fig. 7. The high magnetic-field measurements made it possible to observe the spin splitting of the Landau levels for $B\perp c_3$ as seen in Fig. 6, on which discussion will be made in Sec. IV.

C. Cyclotron resonance

Figure 8 shows the magnetic-field dependence of the infrared transmission for $Bi_{1.48}Sb_{0.52}Se_3$ at a laser wavelength
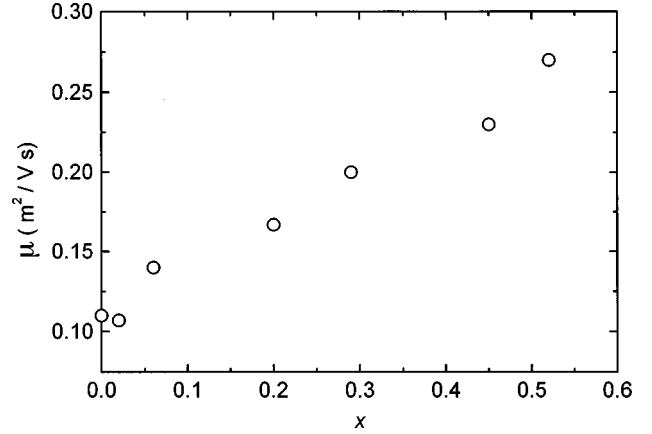
of $\lambda = 10.6$ μm at different temperatures. The transmission at zero field was set as 1.0 for $T = 32$ K. All the other curves were shifted vertically for clarity. The traces shown in Fig. 8 exhibit two peaks at low temperatures. The peaks are relatively broad because of the low mobility of carries. The low-field peak (peak 1) has a larger intensity than the high-field peak (peak 2). As the temperature is increased, peak 2 diminishes rapidly and becomes almost indiscernible at 180 K. As shown in Fig. 9, the same two peaks were observed in all the samples.

The magnetic-field positions of the two peaks were increased as the photon energy was increased. In Fig. 8 experimental traces are shown for $\lambda = 10.6$ μm and $\lambda = 9.25$ μm at two close temperatures 40 and 32 K. The minimum at higher fields disappeared when temperature increased. All the traces are reproducible for magnetic-field sweeps up and down as shown by arrows in Fig. 8. The slight difference in transmission for up and down sweeps is due to temperature rise of samples during the pulse, namely the eddy current effect of the rapid field change in highly conducting samples. This was confirmed by measurements in a long pulse magnetic field (~ 20 ms duration) up to 40 T. Thus we can identify both of the two peaks as the cyclotron resonance. The peak position of the absorption spectra at $T = 32$ K provides effective masses $m^* = 0.075m_0$ and $m^* = 0.105m_0$. It should be noted that these effective masses showed almost no dependence on temperature or electron concentration.

TABLE II. The main frequency of Shubnikov–de Haas oscillations $F_1 = [\Delta(1/B)]^{-1}$, Fermi energy E_F, SdH effect electron concentration n_{SdH}, Hall concentration $1/eR_H$ at $T = 300$ K, thermopower α at $T = 300$ K, and anisotropy $\eta = S_{B\perp C}/S_{B\|C}$ of the Fermi surface for $Bi_{2-x}Sb_xSe_3$ single-crystal samples (extrapolated values of η labeled by $*$).

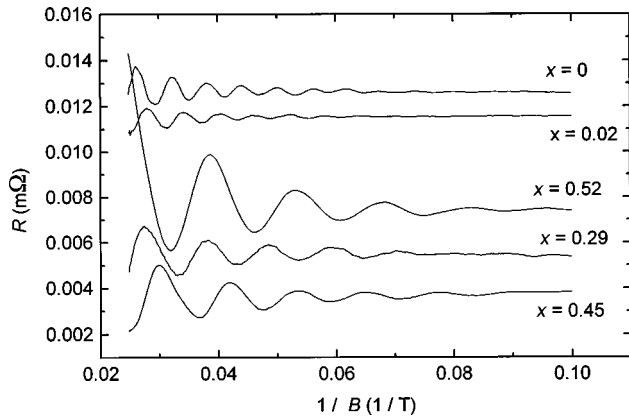| N	x	$[\Delta(1/B)]^{-1}$ (T)	E_F (meV)	n_{SdH} (10^{19} cm^{-3})	$1/eR_H$ (10^{19} cm^{-3})	η	α (μV/K)
1	0	168.3	161.8	2.242	3.67	1.8	57
2	0.02	167.8	161.4	2.238	4.13	1.8*	54
3	0.06	138.5	132	1.84	2.58	1.6*	46
4	0.2	115.1	110	1.0	2.01	1.43*	73
5	0.29	94.2	90	0.67	1.24	1.28	87
6	0.45	85.7	82	0.56	1.03	1.24*	98
7	0.52	70.1	67	0.31	0.84	1.13	108

FIG. 4. Oscillatory part of Shubnikov−de Haas oscillations for different $Bi_{2-x}Sb_xSe_3$ samples as a function of $1/B$ at $T=4.2$ K. Each curve is shifted vertically for clarity.

Figure 9 shows cyclotron resonance traces for $Bi_{2-x}Sb_xSe_3$ with different x. A remarkable feature is that the resonant fields do not depend on x, and, hence on electron concentration.

IV. DISCUSSION

A. Concentration of free electrons

The results of the measurements of the resistivity ρ (Fig. 1 and Table I), the Hall coefficient R_H (Fig. 2 and Table II) and the Seebeck coefficient α (Table II) revealed a presence of minimum around a Sb concentration $x=0.02$ in $Bi_{2-x}Sb_xSe_3$. R_H ($B\|c_3$), ρ in the basal plane and α ($\nabla T \perp c_3$) first decrease as x is increased from zero, and then at larger values of x their magnitudes increase. In other words, the substitution of Bi in Bi_2Se_3 by Sb in the region of small concentrations of Sb results in increase of the concentration of free electrons n, while at higher Sb concentration the value of n decreases. A similar effect has been reported in Ref. 8 on $Bi_{1-x}In_xSe_3$, where the substitution of Bi by In increases the concentration of free electrons for low In content x but decreases it for larger content with increasing x. The concentration of free carriers in Bi_2Se_3 and $Bi_{2-x}Sb_xSe_3$ crystals is determined by lattice point defects. The undoped
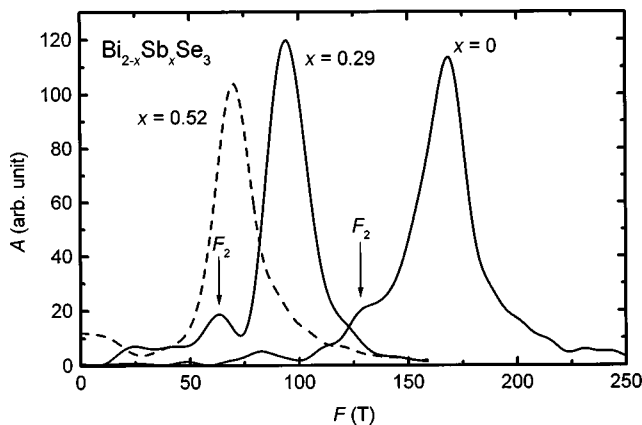

FIG. 5. Fourier transform of the SdH oscillations for B parallel c_3 axis for three samples $Bi_{2-x}Sb_xSe_3$ with different x. Arrows mark the second frequency F_2.
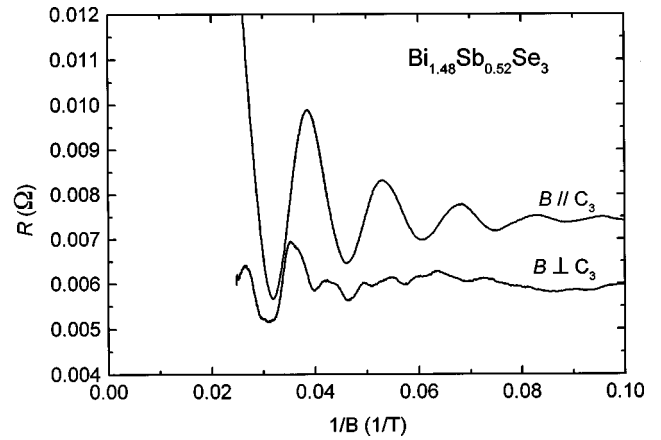

FIG. 6. Oscillatory part of Shubnikov−de Haas oscillations of $Bi_{1.48}Sb_{0.52}Se_3$ sample at $T=4.2$ K for two orientations of magnetic field B: $B\|c_3$ and $B\perp c_3$.

Bi_2Se_3 crystals prepared from the melt of stoichiometric composition always show a superstoichiometric bismuth content.[19] Hence the $Bi_{2+\delta}Se_3$ crystals has n-type electrical conductivity, which is explained by the presence of positively charged vacancies in the selenium sublattice. The excess Bi in these crystals also gives rise to a formation of antisite defects replacing Se atoms by Bi in their lattice sites and having one negative charge. In the low Sb concentration range, the increase of Sb content suppresses the concentration of antisite defects and thus the free-electron concentration increases. The decrease of the electron concentration in the region with higher Sb content is probably associated with the decrease of the concentration of vacancies. Therefore we suppose that the observed change of the concentration of free electrons with increasing x in $Bi_{2-x}Sb_xSe_3$ single crystals is explained by the suppression of the concentration of Se vacancies and elimination of antisite defects. It should be noted that within the accuracy of a few percent, the electron concentration can be controlled reproducibly by varying the Sb content in samples made from different ingots.

B. Spin splitting

The high magnetic-field measurements made it possible to observe the spin splitting of the Landau levels for $B\perp c_3$ as
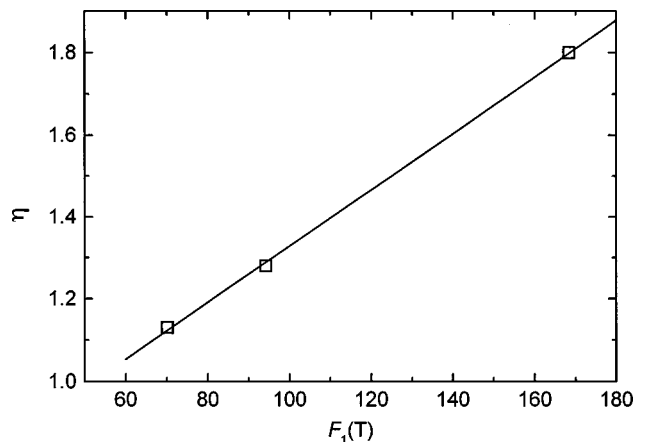

FIG. 7. The ratio $\eta = S_{B\perp C}/S_{B\|C}$ of extremal cross sections of Fermi surface for two different orientation of magnetic field B over the main frequency of SdH oscillations F_1.
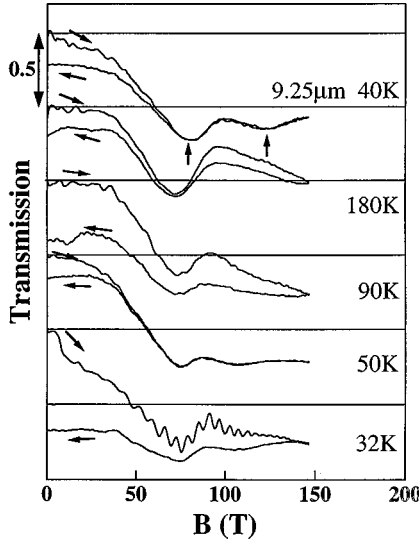
FIG. 8. Transmission traces for $Bi_{1.48}Sb_{0.52}Se_3$ sample versus magnetic field at different temperatures. Arrows show magnetic field sweep up and down.

FIG. 9. Transmission traces for $Bi_{2-x}Sb_xSe_3$ samples with different x versus magnetic field at different temperatures. Wavelength of radiation was 10.6 μm except for the top trace where it was 9.25 μm. Arrows show magnetic-field sweep up and down. The thick arrows indicate the two peak positions (peak one and peak two); d is the thickness of samples.

seen in Fig. 6. The experimental results indicated that the ratio γ of the spin splitting to the orbital splitting was ≈ 0.46. Since $\gamma = gm^*/2m_0$, the value of g factor for electrons in the lower conduction band can be determined, if the effective mass is known for a magnetic field $B \perp c_3$. In this orientation, the present data revealed that the energy spectrum as well as the anisotropy of the Fermi surface is strongly non-parabolic and the effective mass depends on the carrier concentration. In the two-band model, the absolute value of $\gamma = gm^*/2m_0$ is unity just as the free-electron case. For most bulk semiconductors and semimetals, it was found that the value of γ is smaller than or equal to one due to the $k \cdot p$ interaction with other energy bands, as is the present case for $Bi_{2-x}Sb_xSe_3$.

For B parallel to the c_3 axis we did not observe spin splitting for high quantum numbers. That is because γ is nearly unity for this magnetic field direction, since the $E(k)$ relation is almost parabolic. At low quantum numbers, only a small shift in the resistivity extrema is observed.[6] This is in contrast to the case of B perpendicular to the c_3 axis, where the $E(k)$ relation is nonparabolic and very complicated, and thus one can expect that γ is different from unity.

C. The energy spectrum

From the frequency of the SdH oscillation $F_1 = 1/\Delta(1/B)$, the extremal cross section S of the Fermi surface in the momentum space perpendicular to the direction of B may be evaluated by a relation

$$S = ehF_1 = eh/\Delta(1/B). \tag{1}$$

According to experimental and theoretical investigations,[3–6,11,14] there are two conduction bands in Bi_2Se_3. However, almost nothing is known about the upper conduction band. The lower conduction band is located at the Γ point of the Brillouin zone and is represented by an ellipsoid elongated in the c_3 direction with a volume V. From the known dependence of the anisotropy η of the el-
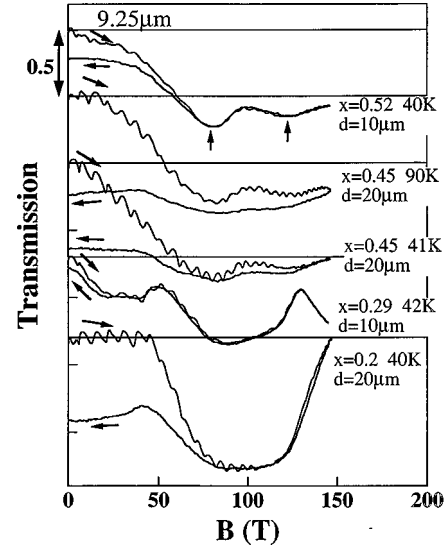
lipsoidal Fermi surface on electron concentration, we can calculate the electron concentration n_{SdH} of the lower conduction band for different x by a simple relation

$$n_{SdH} = 2V/h^3 = \{2 \times 4 \, \eta S_{B \| C3} (S_{B \| C3})^{1/2}\}/\{3(\pi)^{1/2}h^3\}. \tag{2}$$

The values of n_{SdH} are listed in Table II for various samples. The electron concentration derived from the SdH effect data is less than the value of $1/eR_H$ listed in Table II. It may be explained if we suppose that the upper conduction band is filled by electrons.

According to the cyclotron resonance data, there are at least two groups of carriers with different effective masses. The larger cyclotron mass $m^*_{cr} = 0.105m_0$ is in a good agreement with the effective mass value $m^*_{SdH} = 0.12 \pm 0.01m_0$ obtained from the temperature dependence of the SdH oscillation and is ascribed to the electrons in the lower conduction band. The smaller cyclotron mass $m^* = 0.075m_0$ is assigned to the electrons in the higher lying second upper conduction band.

As both effective masses do not depend on carrier concentration it is possible to use simple parabolic dispersion relation to calculate the Fermi energy from the Shubnikov–de Haas effect data:

$$S_{B \| C3} = \pi p^2_{\perp F} = 2 \pi m^* E_F, \tag{3}$$

where $p_{\perp F}$ is the Fermi momentum in the direction perpendicular to the magnetic field. From the experimentally determined $S_{B \| C3}$ and m^*, E_F was calculated for the lower conduction band, and listed in Table II.

Using the Hall-effect data, we plot in Fig. 10 the dependence of the second frequency F_2 as a function of $1/eR_H$. Extrapolation shows that the filling of the second band begins at around $1/eR_H \approx 7 \times 10^{18}$ cm^{-3}.
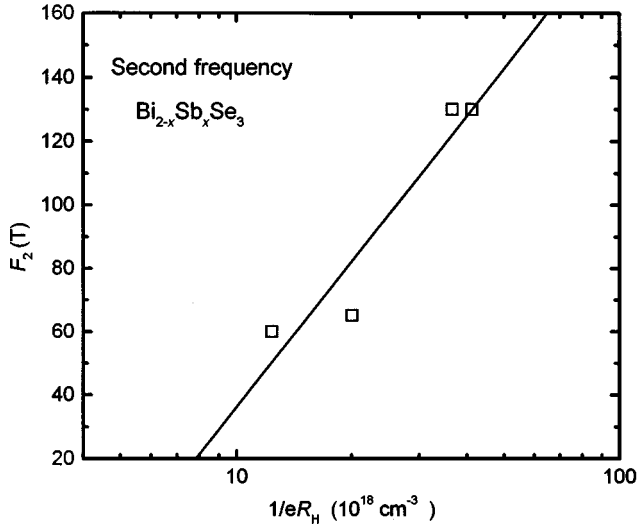
FIG. 10. Dependence of the second frequency of SdH oscillation on $1/eR_H$ in semilogarithmic scale. The straight line is approximation to zero value.

Setting $k=0$ at the center of the Fermi surface, the $E(k)$ relation up to the order of k^4 is represented as

$$E(k)=Ak_\perp^2+Bk_z^2+Ck_z^2k_\perp^2+Dk_z^4+Gk_zk_y(k_y^2-3k_x^2). \quad (4)$$

Here k_z is in the trigonal axis (c_3 axis) in the k space, $k_\perp=(k_x^2+k_y^2)^{1/2}$ is in the perpendicular direction to k_z, k_x is in the binary axis (c_1 axis), and k_y is perpendicular to k_z and k_x. In the formula (4), the term $k_\perp^4$ is omitted, because according to the experimental data the cyclotron mass for $B\|c_3$ does not depend on the energy. The term $Gk_zk_y(k_y^2-3k_x^2)$ accounts for the trigonal warping of the Fermi surface. From the cyclotron resonance data for $B\|c_3$, the value of A can be determined as $A=0.36\times10^{-12}$ meV cm^2. Assuming that the nonparabolicity is negligible for sample Bi$_{1.48}$Sb$_{0.52}$Se$_3$ with the lowest electron concentration, the value of B is calculated from the value of A and the SdH frequency for $B\|c_3$ and $B\perp c_3$: $B=0.28\times10^{-12}$ meV cm^2. For samples with higher electron concentration, the value of B is obtained as $B=0.11\times10^{-12}$ meV cm^2 under the same assumptions. The coefficients C, D, and G depend on the Fermi energy E_F or electron concentration. To determine these coefficients, we need to measure the angular dependence of the Fermi surface which is unknown. For low values of E_F, the density-of-state mass m_d is constant assuming a parabolic band. For one type of carriers,

$$m_d=(3n/16)^{2/3}(1/2)^{1/3}h^2/E_F. \quad (5)$$

For the lower conduction band, our experimental data give $m_d=0.123m_0$. For the upper conduction band the density-of-state mass should be of the order of $0.11m_0$. The energy splitting of the lower and higher bands is about $\Delta E=40$ meV. For a sample with $x=0.02$ the value $1/eR_H$ appears to be a factor 1.85 larger than the SdH density according to Table II. In the cyclotron resonance experiments, we observed two groups of carriers with different masses. Thus we may ascribe this deviation in electron concentration to the electrons in the upper conduction band. The larger mass measured by cyclotron resonance ($m^*=0.105m_0$) corresponds to the lower conduction band and the light effective mass ($m^*=0.075m_0$) to the upper conduction band. We observed a single SdH frequency for $B\perp c_3$ and it is not possible to calculate the electron concentration in the upper band. Some fraction of electrons might be created also by a contribution of the impurity band with low mobility carriers. At the moment we cannot exclude fully the possibility of impurity band.

Thus we can consistently explain the SdH effect and cyclotron resonance data by existence of two conduction bands. The open question still remains concerning why the intensity of the second frequency F_2 in SdH oscillation is less than F_1.

V. CONCLUSION

Cyclotron resonance was observed in Bi$_{2-x}$Sb$_x$Se$_3$ single crystals for magnetic field B parallel to the c_3 axis. Cyclotron resonance data revealed two groups of carriers with different effective masses which do not depend on the carrier concentration or temperature for $B\|c_3$. This gives an evidence of the parabolic energy spectrum for this orientation of magnetic field and concentration range of electrons. On the other hand, the SdH data of the anisotropy of the Fermi surface revealed a strong nonparabolic energy spectrum for $B\perp c_3$ as the anisotropy factor strongly depends on the electron concentration.

[1] U. Birkholz, in *Amorphe und Polykristalline Halbleiter*, edited by W. Heywang (Springer-Verlag, Berlin, 1984), p. 77.
[2] *Thermoelectric Materials—New Directions and Approaches*, edited by T. M. Tritt, M. G. Kanatzidis, H. B. Lyon, Jr., and G. D. Mahan, MRS Symposia Proceedings No. 478 (Materials Research Society, Pittsburgh, 1997).
[3] H. Kohler, Phys. Status Solidi B **58**, 91 (1973).
[4] H. Kohler, Solid State Commun. **13**, 1585 (1973).
[5] H. Kohler and H. Fisher, Phys. Status Solidi B **69**, 349 (1975).
[6] H. Kohler and E. Wuchner, Phys. Status Solidi B **67**, 665 (1975).
[7] J. Horak, L. Koudelka, J. Klikova, and L. Siska, Phys. Status Solidi A **11**, 575 (1982).
[8] R. Novotny, P. Lostak, and J. Horak, Phys. Scr. **42**, 253 (1990).
[9] V. A. Kutasov, L. N. Luk'yanova, P. P. Konstantinov, and G. T. Alekseeva, Fiz. Tverd. Tela (St. Petersburg) **39**, 483 (1997) [Phys. Solid State **39**, 419 (1997)].

[10] V. A. Kulbachinskii, Z. M. Dashevskii, M. Inoue, M. Sasaki, H. Negishi, W. X. Gao, P. Lostak, J. Horak, and A. de Visser, Phys. Rev. B **52**, 10 915 (1995).

[11] V. A. Kulbachinskii, N. Miura, H. Nakagawa, H. Arimoto, T. Ikaida, P. Lostak, and C. Drasar (unpublished).

[12] S. Katsuki, J. Phys. Soc. Jpn. **26**, 58 (1969).

[13] E. V. Oleshko and V. N. Korolyshin, Fiz. Tverd Tela (Leningrad) **27**, 2856 (1985) [Sov. Phys. Solid State **27**, 1723 (1985)].

[14] P. Pecheur and G. Toussaint, J. Phys. Chem. Solids **55**, 327 (1994).

[15] E. V. Oleshko and V. N. Korolyshin, Fiz. Tekh. Poluprovodn. **19**, 1839 (1985) [Sov. Phys. Semicond. **19**, 1130 (1985)].

[16] V. G. Kuznetsov, K. K. Palkina, and A. A. Reshchikova, Izv. Akad. Nauk SSSR, Neorg. Mater. **4**, 670 (1968) [Inorg. Mater. **4**, 585 (1968)].

[17] K. Nakao, F. Herlach, T. Goto, S. Takeyama, T. Sakakiba, and N. Miura, J. Phys. E **18**, 1018 (1985).

[18] N. Miura, in *Infrared and Millimeter Waves*, edited by K. J. Button (Academic, New York, 1984), Vol. 12, p. 73.

[19] G. Offergeld and J. Van Carenberghe, J. Phys. Chem. Solids **11**, 310 (1959).